Effects of Annealing Process on the WO_3 Thin Films Prepared by Pulsed Laser Deposition

To cite this article: Ali A. Yousif and Ameer I. Khudadad 2020 *IOP Conf. Ser.: Mater. Sci. Eng.* **745** 012064

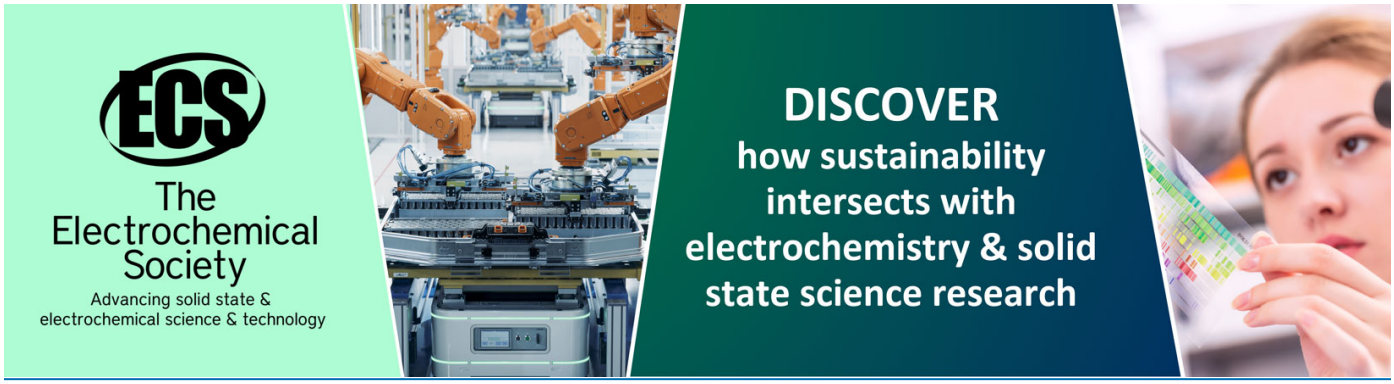

IOP Conf. Series: Materials Science and Engineering **745** (2020) 012064 doi:10.1088/1757-899X/745/1/012064

Effects of Annealing Process on the WO_3 Thin Films Prepared by Pulsed Laser Deposition

Ali A. Yousif[1], Ameer I. Khudadad[2]

[1]University of Mustansiriyah
[2]University of Mustansiriyah, E. mail:ameerib7771@gmail.com

Abstract: This work presents a study of the effect of annealing temperature on the optical and structural properties of WO_3 that has been deposited by Pulsed Laser Deposition (PLD) method at 300°C on the rules of glass and indicates the effect of annealing temperatures 350, 450 and 550°C for one hour on those properties. The results of X-Ray diffraction showed all the films prepared with the installation of multi-crystalline tetragonal and directional prevalent (010) for all models after annealing. The annealing led to an increase in the grain size. Full width at half maximum FWHM values of the (010) peaks of these films decreased from 1.492° to 1.064° with increasing annealing temperature, and the highest value of the specific surface area was 63 m^2/gm. The natural structure of the WO_3 nanoparticles films were studied by using field emission scanning electron microscopy (FESEM), it revealed that the average grain size increased with increasing of annealing temperature from 46.57 to 485.1nm. The optical features of the films were studied by Photoluminescence PL, the results gave one emission peaks located at 437 nm, and there was a red shift when the annealing temperatures were increased.

1. Introduction

There are some allotropic modifications, such as tetragonal, monoclinic and orthorhombic structure that could be seen for tungsten oxide thin films. Researchers pointed out that these structures are affected by many factors, including temperature, impurity and substrate material. Tungsten oxide WO_3 films are n-type semiconductors with an energy band gap of 2.8 eV [1] having a strong absorption within the solar spectrum of 440 nm. These films have been widely studied for various applications such as photocatalysis [2], high density memory devices, smart windows [3], gas sensor [4], photoelectrochemical water splitting, and electrochromism [5,6]. Generally, the characterization of thin films is carried out by using different tools, like x-ray diffraction [7] and field emission-scanning electron microscopy [8]. The general properties, such structure, composition, surface morphology and band gap of thin films can be investigated. Several techniques, such as spin coating, colloidal, electrophoretic deposition chemical and physical vapor deposition can be used. Electrophoretic deposition (EPD) provides an easy and reliable coating technique, where the charged particles suspended in the solution are attracted to the electrode surface under the influence of an electric field [9]. Almost all the oxide-based (EC) devices employ tungsten oxide [10].

In this work, nanoparticle WO_3 films have been deposited on a glass substrate by using PLD method with a sputtering pressure of 10^{-2} mbar and annealed at 350, 450 and 550^{o}C. The surface morphological, structural, and optical features of nanostructured WO_3 films have been investigated and discussed.

2. Experimental work

The precipitation was executed utilizing a second harmonic generation SHG Nd:YAG Q - switched laser at a wavelength of 532 nm with repetition rate 6 Hz and pulse width 7 nsec. The deliberated films were fabricated using pure WO_3 nanoparticles targets. WO_3 films were grown on glass substrates by pulsed laser deposition at a distance of 10 cm from the target. A rectangular glass substrates of rib length of 2 cm WO_3 with purity of 99.99% have been selected from one of the well-known international company producing this material, then taking 3 grams of $WO_3$and putting inside a press to obtain a hard disc, which is regarded as a target and will be held in the instruments, chamber and bombarded by pulsed laser. During the deposition, the chamber was retained at vacuum pressure of 10^{-2} mbar, while the substrate temperature (T_s) was set at 300°C, laser influence at 2.64 J/cm^2 and 700 numbers of pulses. For the purpose of knowing the type of the crystal structure of any material, X-Ray diffraction technique was used, where the samples were examined by a device XR-DIRACTOMETER/6000 of the type Shimadzu. To measure the particle or grain size for all samples, SEM technique was used, type T EASCAN manufactured by a company UEGA. LM of Geck origin. The EDS measurement confirmed the wt % of individual elements and the absence of impurities. The PL Photolummince was carried out via Perkin-Elmer luminescence spectrometer model: LS55 equipped with a xenon flash lamp.

3. Results and Discussion:

Through the X-Ray diffraction measurements, a complete analysis of the X-Ray diffraction is conducted and what represents each of the forms and changes that occurred, as well as it was conducted to identity the nature of crystalline and synthetic growth of the crystal and the stages in which the prepared material. X-Ray spectrum is greatly influenced the preparatory conditions, which have the effect of completing crystalline growth. XRD patterns of the tungsten oxide nanoparticles heat treated at 350, 450 and 550 ^oC are depicted in Figures 1a to 1c. Figure 1a. demonstrates the polycrystalline structure of tungsten oxide nanoparticles for the sample that heat treated at 350 ^oC. In the samples that exposed to the elevated temperature of annealing of 450 ^oC as shown in Figure1b. the creation of triplet peaks has been detected, and revealed the well oriented and high intensity of the quality of the crystalline. The obtained phases were compatible to ICDD card no. 5-0386 which they correspond to the crystalline structure of monoclinic. Furthermore, the construction of predominant triple peaks of 010 progress directions displays the structure of monoclinic, polycrystalline phase and texture progression of the samples heat treated at 350^oC to 550 ^oC, elucidated that the samples were growing along the axes a, b, and c, correspondingly approving the textured growth and columnar of the samples. The strong sharp peaks in X-Ray diffraction pattern emphasize the stoichiometry and crystallinity of the tungsten oxide nanoparticles. The nature of single phase of the samples was likewise definite from the existence of X-Ray diffraction peaks relating to the tungsten oxide phase only. By increasing the temperature of annealing, the diffracted peaks intensity grows into high intensity and high degree of sharpness. The boosted preferential orientation after heat treatment at elevated degree of temperatures could be attributed to the atoms that moving along the surface of the substrate to touch the weak energy nucleation sites and rising preferentially there itself. After interpreting the previous figures, it can be concluded that the crystalline structure is affected by changes of the heat treatment temperature; the thin film generally depends on the sedimentation temperature, the type of precipitated base and the temperature changes as well as other decomposition factors. And, the results of X-Ray diffraction explained the variation in crystalline levels, where the compressive stresses generated in the sample as a result of the preparation method play a role to change the peaks of brag. As well the temperature difference plays a role in the composition of crystalline levels whether monocrystalline or multi-crystalline or random crystalline inaddition to the dependence on the type of precipitated base .The reasons for the low rate of crystallization can be due to the type of nucleus formed between the atoms of the thin film material or because at the specific heat at the solid body [11] or because of different melting points of the components of the material or thermodynamic properties of the mixture which are consistent with the reference [12]. The crystallization of the thin film greatly affects many properties, including the gap energy of the crystalline material [13]. The crystalline size was calculated using the Scherrer formula1 [14].

$$D = 0.94\,\lambda / [L_{2\theta} \cos\theta] \quad (1)$$

Where
D: crystalline sizes
θ: angle between plans
λ: wavelength of X-Ray of Cu Kα radiation which equals to 1.540 Aº
L: pulse width at half maximum of diffraction peaks.

The average crystalline sizes of tungsten oxide nanoparticles samples annealed at 350, 450, and 550ºC were obtained by utilizing formula and were about 13.11, 18.48, and 21.4 nm, respectively, which define the nature of nanocrystalline of the samples. Table 1. elucidates that the crystalline size increased as the temperature of annealing is increasing [15]. The specific surface area S.S.A of WO_3 nanoparticles is given by equation 2 [16].

$$S.S.A = 6000 / D * \rho_d \quad 2$$

Where ρ is the density of WO_3 nanoparticles and it is calculated based on the density of WO_3 by taking into account the percentage of elements in EDS analysis. Table 1 also shows the value of 2θ, FWHM, Crystalline size, and Surface area for annealing temperature 350, 450, and 550ºC.

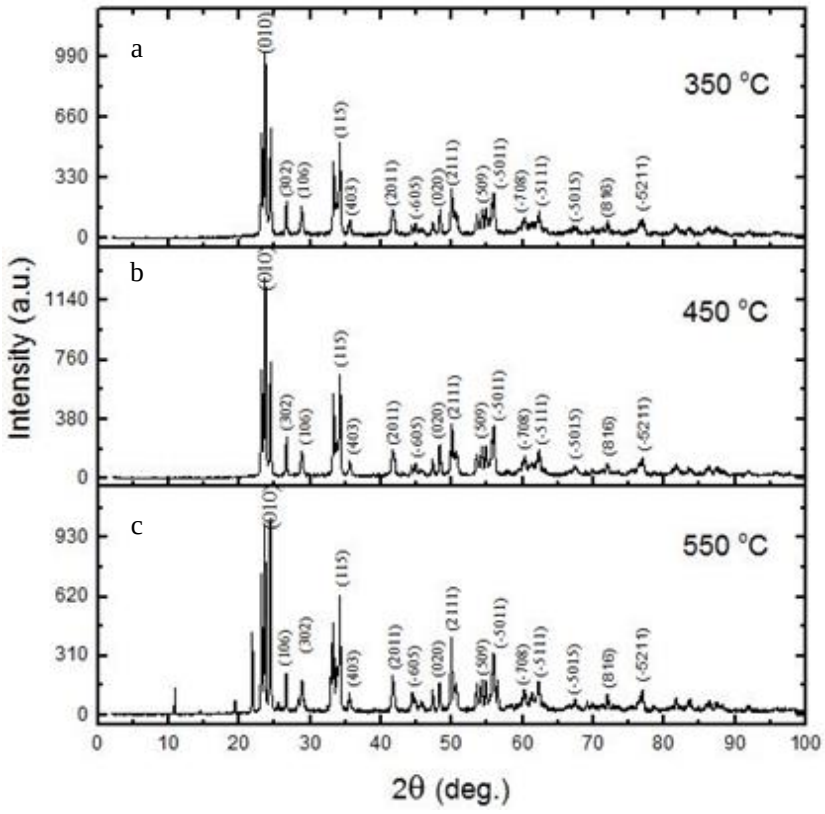

Figure 1: XRD diffraction of WO_3 films at different annealing temperatures.

Table 1: XRD properties.

Sample	2θ	FWHM	Crystalline size nm	Surface Area gm^2/cm
350ºC	24.75	0.62	13.11	63.56
450ºC	24.71	0.44	18.48	45.09
550ºC	24.85	0.38	21.40	38.94

4. Structure analysis

The surface of the deposited thin film as well as the effect of annealing temperature on these prepared thin film were studied in the same preparation conditions, and the changes on these surfaces were observed through field the emission-scanning electron microscopy FE-SEM technique, which gives very accurate and clear shapes that reach very high magnification, and has the ability to calculate the average grain size of these surfaces. The action of thermal retrogression at 350ºC could be noted in the FESEM images that indicated in Figure 2. The images displayed a highly brittle, very dense aggregated nanoparticles and nanorods shape.

The nanorods present the widths of nanometers and the lengths of some microns. However, higher annealing temperature of 450ºC leads to the materialization of agglomerated clouded WO_3 nanoparticles as revealed in the Figure 2b. No insights of nanorods are recognized confronting to the development of nanoparticles at the overhead of nanorods. When the annealing process at different temperatures achieved on the samples, it was noticed that the annealing resulted in the clarity of the characteristics of the grain size of the samples and varied among the samples. It ca be seen that the clarity starts from lower grades to higher grades, which are 550^{o}C and as shown in Figure 2c. where the shape of nanoparticles is dictated by their edges leading to squared or hexagonal-like nanoparticles.

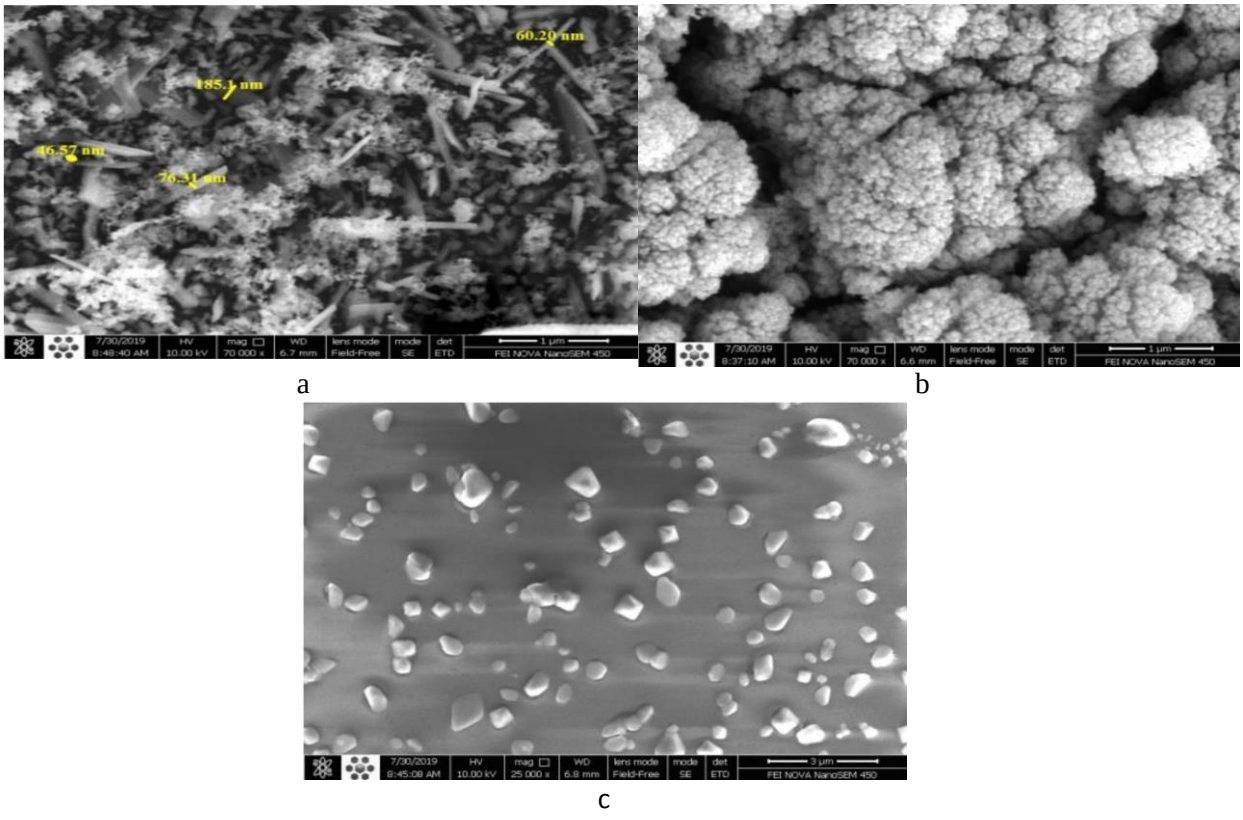

Figure 2: FE-SEM images for WO_3 nanoparticles at annealing temperature at a. 350 °C, b. 450 ^{o}C and c. 550^{o}C.

EDS technique was used to know the approximate percent are of the element which the thin film formed from the inspections that were out carried for each annealing temperature for all samples. It was shown from the Figures 3a. 3b and 3c. that the percentage of W nanoparticles is much higher than (O) even that after annealing, and Figures 4a., 4b., and 4c. reveals that the elemental mapping has no impurities with the (W) and (O) elements, were (W) represents by blue particles and (O) by red particles .

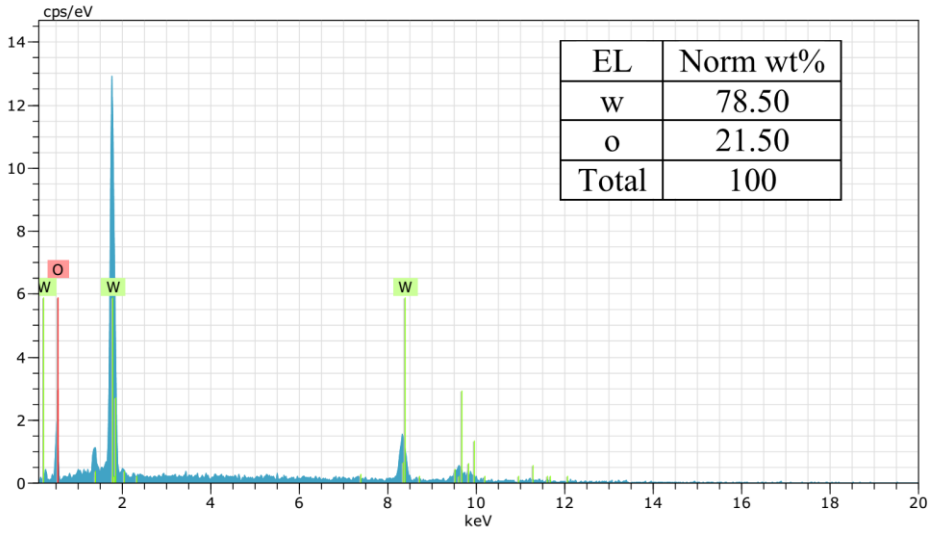

EL	Norm wt%
w	78.50
o	21.50
Total	100

a

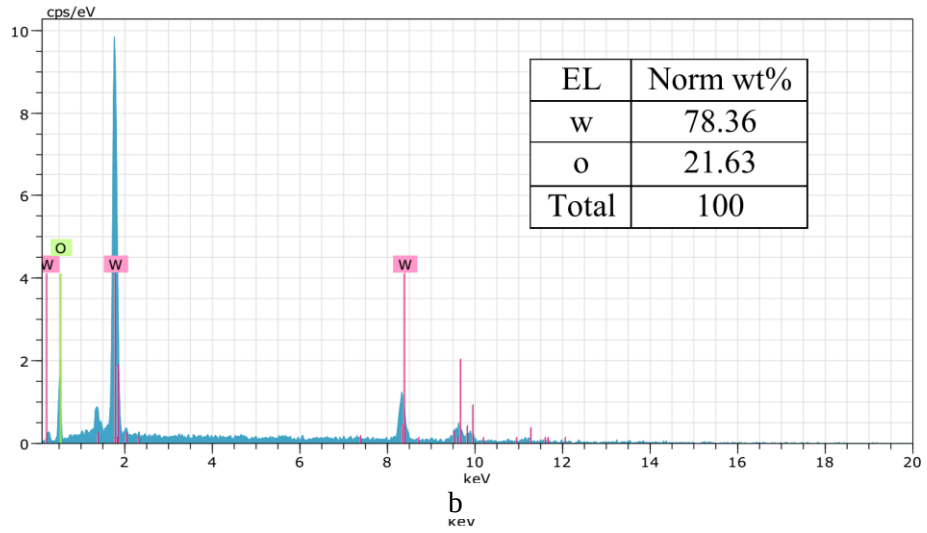

EL	Norm wt%
w	78.36
o	21.63
Total	100

b

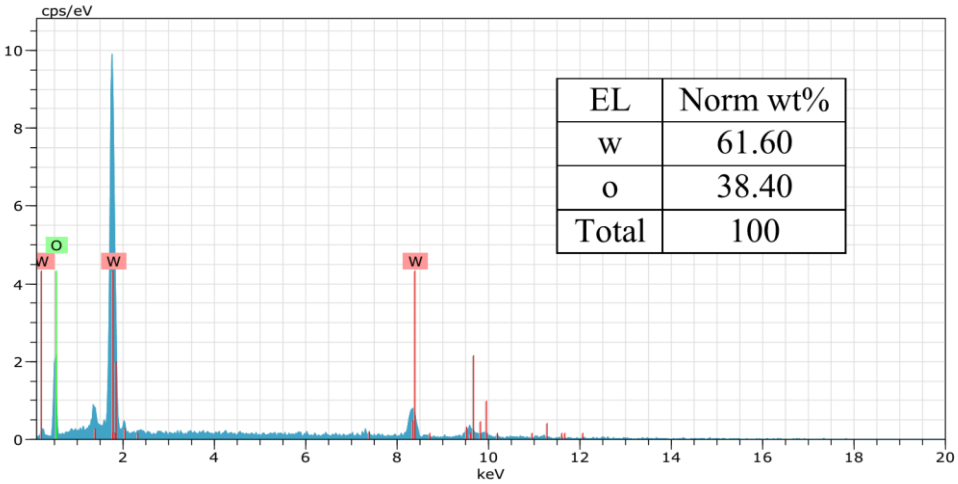

EL	Norm wt%
w	61.60
o	38.40
Total	100

c

Figure 3: EDS graph showing the quantitative values of elements present in the WO_3 nanoparticles at annealing temperature a. 350 °C, b. 450°C, and c. 550°C

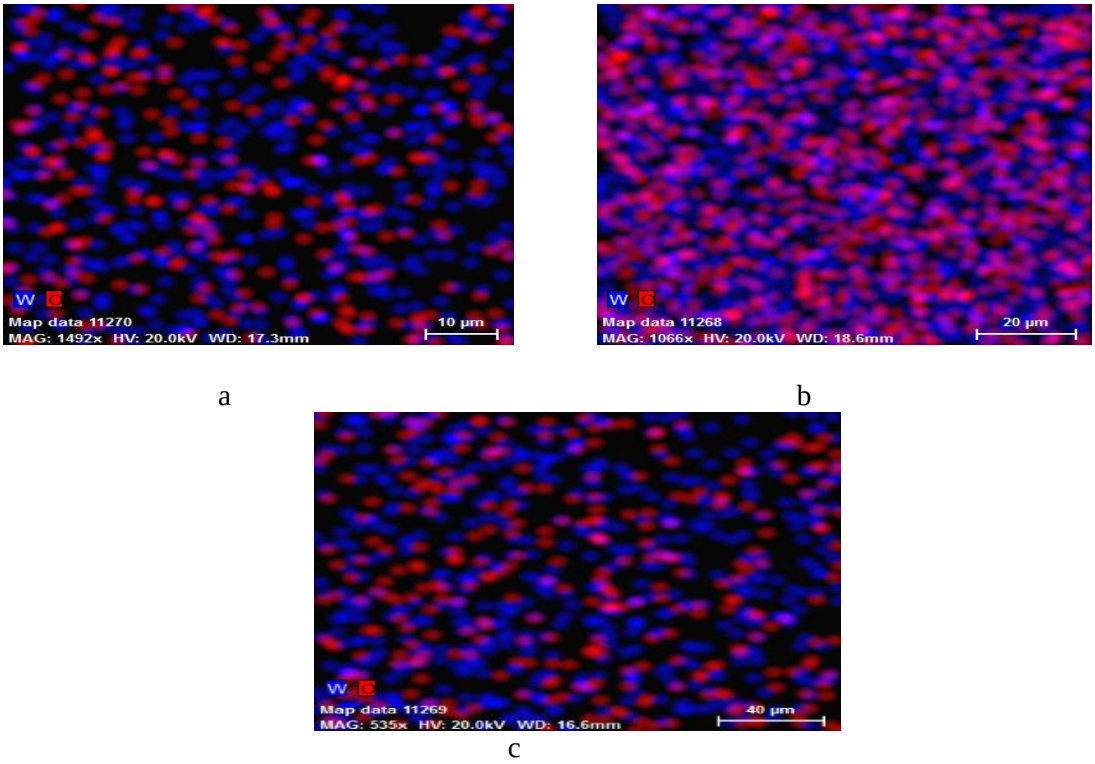

Figure 4: Distribution of WO_3 nanoparticle and elemental mapping at the annealing temperature a. 350^{o}C, b. 450^{o}C and. c 550^{o}C.

5. Optical Properties:

The Photolummince PL spectra of WO3 samples are visible PL spectra region, as shown in Figure 5. The excitation wavelength was 225 nm. The sample that annealed at 350^{o}C has a peak centered in 437 nm wavelength with an energy gap of 2.83 eV. There is a red shift when the annealing temperatures were increased, this can be attributed to the growth of grain size. The energy gap is listed in table 2.

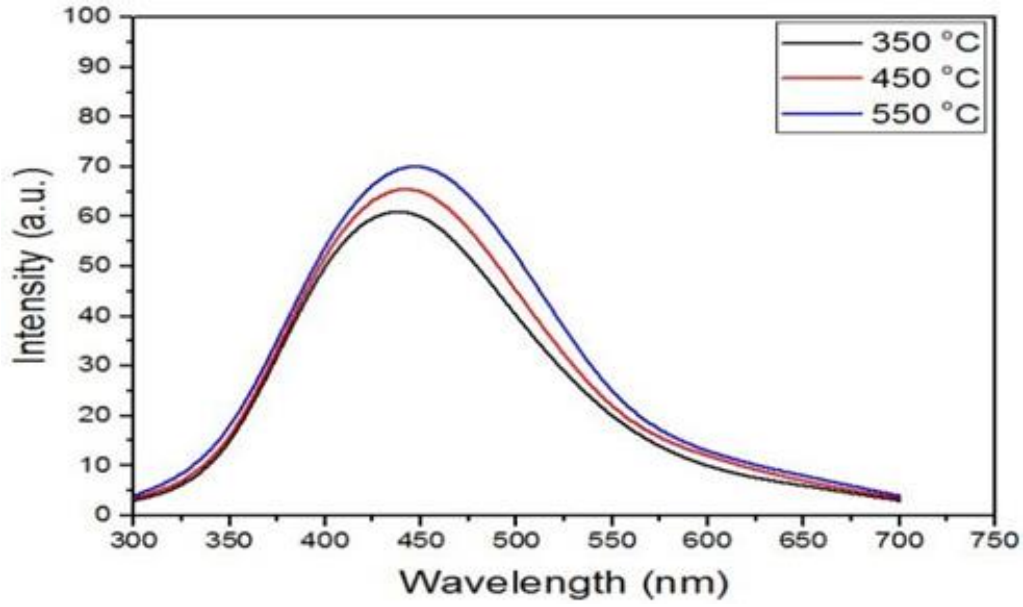

Figure 5: Room-temperature photoluminescence of the WO_3 thin films as-deposited and annealed at different temperatures.

Table 2: The value of annealing temperature, wavelength, and energy gap.

Annealing Temperature °C	Wavelength nm	Energy gap eV
350	437	2.82
450	441	2.81
550	446	2.78

6. Conclusion

XRD investigation evidently elucidates the creation of the main triple peaks of (010) growing directions, which reveal the textured growth nature, monoclinic, and polyphase of the samples annealed at 350 to 550^{o}C. Well oriented, high intensity with the development of crystalline quality of the samples was noticed when the annealing temperature was increased. The highly oriented growth and excellent aligned peaks itemize the stoichiometric nature of the samples. Greater annealing temperature enriches the growing of oriented nanocrystalline samples and reductions of the energy band gap to 2.78 eV. FE-SEM features depicted that the thermal progression of WO_3 nanoparticles samples are described by a morphological transformation, where WO_3 nanorods go to the aggregated spherical WO_3 nanoparticles at a temperature of 450^{o}C and turn into nanocubic-like structures at a temperature of 550°C. The outcomes of this work presented that the Pulsed Laser Deposition technique is a very promising method which is evident at low synthesis temperature, short production time, low cost, and leading to materials with high homogeneity and purity. The efficient structural and optical investigations mani Fested the high potential of this technique on the WO_3 nanoparticles and future technological applications.

References

[1] Hunge, Y. M., Mahadik, M. A., Kumbhar, S. S., Mohite, V. S., Rajpure, K. Y., Deshpande, N. G., & Bhosale, C. H. 2016. Visible light catalysis of methyl orange using nanostructured WO_3 thin films. *Ceramics International*, *42*1, 789-798.

[2] WL Kwong, A Nakaruk, P Koshy, and C C Sorrell 2013. Photoelectrochemical properties of WO_3 nanoparticulate thin films prepared by carboxylic acid-assisted *electrode position* 544, 191-196.

[3] Shen, Y., Pan, L., Ren, Z., Yang, Y., Xiao, Y., & Li, Z. 2016. Nanostructured WO3 films synthesized on mica substrate with novel photochromic properties. *Journal of Alloys and Compounds*, *657*, 450-456.

[4] LE Jose, AR Manuel, M Jose,and H Abel 2016. *Microstructure and mechanical properties of sputter-deposited nanocrystalline w1-ymoyo$_3$thin films*, master thesis, University of Texas at El Paso.

[5] A Karuppasamy 2013. Electrochromism in surface modified crystalline WO3 thin films grown by reactive DC magnetron sputtering . *Applied Surface Science*, *282*, 77-83..

[6] Ho, S. M. 2016. Preparation and characterization of tungsten oxide thin films. *Journal of Chemical and Pharmaceutical Research*, *8*7, 414-416.

[7] Carreón-Moncada, I., González, L. A., Pech-Canul, M. I., & Ramírez-Bon, R. 2013. Cd1−xZnxS thin films with low Zn content obtained by an ammonia-free chemical bath deposition process. *Thin Solid Films*, *548*, 270-274.

[8] KD Lee, S Seo, D Lee, H Kim, J Jeong, MJ Ko, B Kim, D Kim, and JY Kim 2013. Preparation and characterization of tungsten oxide *Thin solid films* 546, 294-298.

[9] M. Yagi, S. Maruyama, K. Sone, K. Nagai and T. Norimatsu 2008. J. Solid State Chem, 181.175.

[10] G.A. Niklasson, C.G. Granqvist 2007 . J. Mater. Chem. Electrochromics for smart windows: thin films of tungsten oxide and nickel oxide, and devices based on these 17.127.

[11] Xilian Sun, Hongtao Cao, Zhimin Liu, and Jianzhong Li 2009 . Influence of annealing temperature on microstructure and optical properties of sol–gel derived tungsten oxide films,

Applied Surface Science 255, 8629–8633.
[12] Y. Takeda, N. Kato, T. Fukano, A. Takeichi and T. Motohiro 2004 .Journal of Applied Physics 96, 2417.
[13] G. Garcia-Belmonte, P. R. Bueno, F. FabregatSantiago and J. Bisquert 2004. Relaxation processes in the coloration of amorphous WO_3WO_3 thin films studied by combined impedance and electro-optical measurements *Journal of Applied Physics* 96, 853
[14] Husam R. Abed, Alwan M. Alwan, Ali A. Yousif, Nadir F. Habubi 2019. Efficient SnO_2 CuO/porous silicon nanocomposites structure for NH_3 gas sensing byincorporating CuO nanoparticles, *Optical and Quantum Electronics* 51,1-13.
[15] Alwan M. Alwan,and Allaa A. Jabbar 2011. Design and fabrication of nanostructures silicon photodiode, *Modern Appl Sci* 5, 106–112.
[16] Duaa A. Hashim, Alwan M. Alwan and Muslim F. Jawad 2018 . investigation of structural properties of monometallic Ag, Pd and Bimetallic Ag@Pd Nanoparticles Growth on Macro Porous Silicon, I*nternational Journal of Nanoelectronics and Materials* 11, 461-472